

# Novel rhenium(V) nitride complexes with dithiocarbamate ligands – A synchrotron X-ray and DFT structural investigation

J Perils et al.,

Author post-print (accepted) deposited by Coventry University's Repository

**Original citation & hyperlink:**

Perils, Joanne, et al. "Novel rhenium (V) nitride complexes with dithiocarbamate ligands—A synchrotron X-ray and DFT structural investigation." *Inorganica Chimica Acta* 475 (2018): 142-149.

<https://dx.doi.org/10.1016/j.ica.2017.11.023>

ISSN 0020-1693

Publisher: Elsevier

**NOTICE: this is the author's version of a work that was accepted for publication in *Inorganica Chimica Acta*. Changes resulting from the publishing process, such as peer review, editing, corrections, structural formatting, and other quality control mechanisms may not be reflected in this document. Changes may have been made to this work since it was submitted for publication. A definitive version was subsequently published in *Inorganica Chimica Acta*, Vol 475, pp. 142-149 (2018)**

© 2018, Elsevier. Licensed under the Creative Commons Attribution-NonCommercial-NoDerivatives 4.0 International

<http://creativecommons.org/licenses/by-nc-nd/4.0/>

Copyright © and Moral Rights are retained by the author(s) and/ or other copyright owners. A copy can be downloaded for personal non-commercial research or study, without prior permission or charge. This item cannot be reproduced or quoted extensively from without first obtaining permission in writing from the copyright holder(s). The content must not be changed in any way or sold commercially in any format or medium without the formal permission of the copyright holders.

This document is the author's post-print version, incorporating any revisions agreed during the peer-review process. Some differences between the published version and this version may remain and you are advised to consult the published version if you wish to cite from it.

## **Novel Rhenium(V) nitride complexes with dithiocarbamate ligands – a synchrotron X-ray and DFT structural investigation**

Joanne Perils<sup>a,b#</sup>, Fernando Cortezon-Tamarit<sup>c#</sup>, Navaratnarajah Kuganathan<sup>d#</sup>,  
Gabriele Kociok-Köhn<sup>c</sup>, Jonathan R. Dilworth<sup>\*b</sup> and Sofia I. Pascu<sup>\*c</sup>

<sup>a</sup> School of Chemistry, University of KwaZulu-Natal, Private Bag X01, Pietermaritzburg, 3209, South Africa

<sup>b</sup> Department of Chemistry, University of Oxford, Chemistry Research Laboratory, South Parks Road, Oxford, OX1 3TA, UK, email: jon.dilworth@chem.ox.ac.uk

<sup>c</sup> Department of Chemistry, University of Bath, Claverton Down, Bath, BA2 7AY, UK, email: s.pascu@bath.ac.uk

<sup>d</sup> Department of Materials, Imperial College London, Royal School of Mines, Exhibition Road, London, SW7 2AZ, UK

**Keywords:** Rhenium(V) nitrides, sulfonamide, dithiocarbimates

---

### **Abstract**

The application of rhenium complexes as therapeutic agents in nuclear medicine has propelled research into the chemistry of these compounds. In our effort to develop and investigate new therapeutic radiopharmaceuticals based on the complexes of rhenium we have investigated the nitride core, [ReN]<sup>2+</sup>. This work looks at the behavior of sulfonamide based dithiocarbimates towards the rhenium(V) nitride core. The aim here was to prepare anionic complexes with aromatic as well as fluorescent aromatic groups in the sulfonamide substituent located on the dithiocarbamate backbone. We envisaged that the polar sulfonamide and dianionic charge would confer solubility in water. Here we report the reactions of the dithiocarbamate ligands towards the rhenium(V) precursors: [ReNCl<sub>2</sub>(PPh<sub>3</sub>)<sub>2</sub>] and [ReNCl<sub>2</sub>(PMe<sub>2</sub>Ph)<sub>3</sub>]. These reactions proceeded with bis-substitution by the dithiocarbamate ligand, resulting in the formation of a dianionic rhenium(V) complex, of the type [ReN(S-S)]<sup>2-</sup>, where (S-S) denotes the sulfonamide-tagged dithiocarbimato unit. Spectroscopic characterization data, as well as the synchrotron X-ray diffraction structure of the metal complex with the phenyl sulfonamide backbone shed light into the structural features of this interesting class of ligands and opens up opportunities for further studies in molecular imaging and therapeutic arenas

## Introduction

Despite significant progress made in the development of diagnostic radioisotopes for medical imaging techniques such as single photon emitted computed tomography (SPECT) or positron emission tomography (PET), the availability of therapeutic radioisotopes with matching radiochemistry, half-lives and wide accessibility at reasonable costs remains the holy-grail for applications in nuclear medicine, particularly for oncology. The development of rhenium compounds as therapeutic radiopharmaceuticals remains a matter of interest for chemists and nuclear imaging specialists both in academic and in clinical settings.

To date, the most widespread use of rhenium complexes in major clinical applications is that involving ReHEDP (hydroxyethane bisphosphonate) for uses in bone targeting in terminal cancer patients [1]. The research area has been reviewed: the chapters in *Comprehensive Coordination Chemistry on Technetium* by Alberto [2] and *Rhenium* by Abram, [3] are detailed. Extensive reviews have covered the recent chemistry aspects of both  $^{186/188}\text{Re}$  and  $^{99\text{m}}\text{Tc}$  chemistry across a whole range of available oxidation states and coordination numbers in aqueous and non-aqueous media [4,5]. Our recent book Chapter also gives an overview of the development of the coordination chemistry of Tc and Re relevant to nuclear medicine with an emphasis on key ligand systems and imaging agents [4].

The strong  $\pi$ -donating characteristics of the trianionic nitride-group make a major contribution to the stability of high oxidation state Tc and Re nitrides. The presence of an additional negative charge on “nitride” compared to “oxo” opens up a series of complexes with different co-ligands, or overall charges, to those of the ubiquitous Re-oxo complexes. Tc or Re nitride syntheses were first carried out by Chatt et al. who showed that  $[\text{ReNCl}_2(\text{PPh}_3)_2]$  and  $[\text{ReNCl}_2(\text{PMe}_2\text{Ph})_3]$  could be synthesized using hydrazine or azide as the source of nitride [6,7]. This work was extended to  $^{99}\text{Tc}$  and  $^{99\text{m}}\text{Tc}$ : Baldas and co-workers reported extensively on nitride complexes and proposed that the nitride core could be used in  $^{99\text{m}}\text{Tc}$  based radiopharmaceuticals [8–14]. The paramagnetic Tc(VI) species  $[\text{TcNCl}_4]^-$  emerges from the reaction between pertechnetate and azide in acid solution. Its substitution and redox chemistry (by the same synthetic route) was applied to the synthesis of  $[\text{ReNCl}_4]^-$  [15]. The coordination chemistries and spectroscopic properties of the  $[\text{TcN}]^{2+}$  and  $[\text{ReN}]^{2+}$  cores were highlighted by Abram et al. and some representative examples of this work are shown in Fig. 1 (A–C) [16–18,15,19]. In the nitride complexes research space, Duatti and co-workers showed that neutral dithiocarbamato-Tc nitrides act as promising heart imaging agents. Particularly, the bis(N-ethoxy, N-ethyl dithiocarbamato)nitrido technetium(V), *TcNOET* (Fig. 1, compound **D**) entered clinical trials despite the fact that myocardial tissue retention remains unclear [20–22].

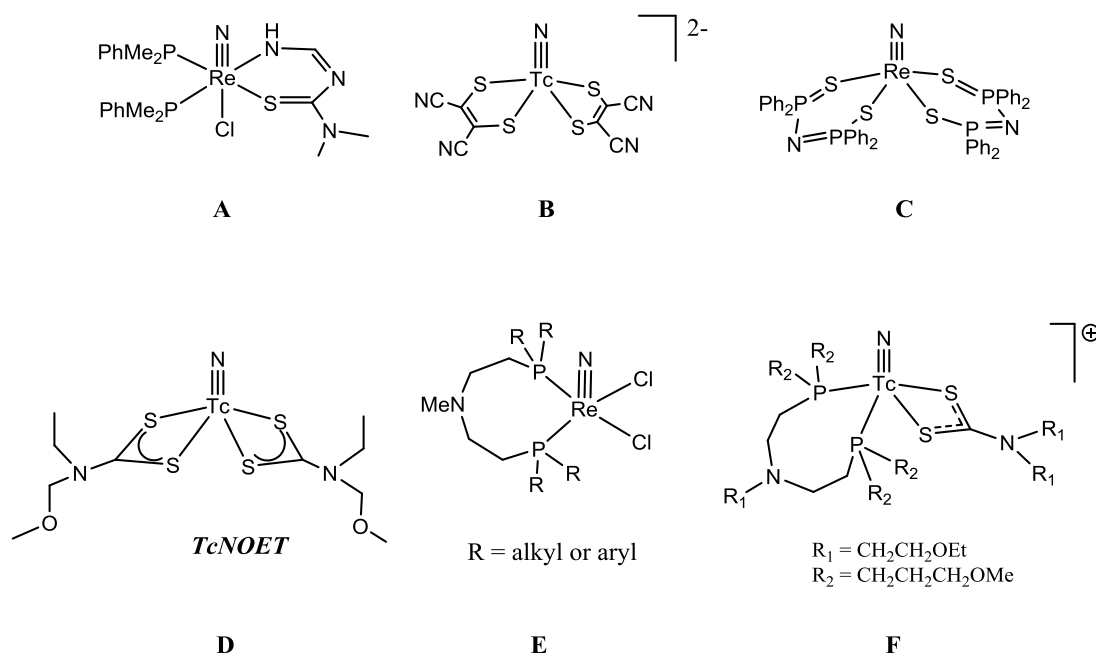


**Figure 1.** Representative examples of complexes exhibiting the TcN and ReN cores.

The hydrazine derivative  $\text{MeSCSNMeNH}_2$  and its variants led to the formation of both  $[\text{TcN}]^{2+}$  and  $[\text{ReN}]^{2+}$  cores directly from the corresponding tetroxometallates in high yields [23,24]. No intermediates could be isolated with the Tc core but the  $[\text{ReO}(\text{NHNMeCSSMe})_2]^+$  species emerged from the reaction of  $[\text{ReO}_4]^-$  with the *N*-methylated hydrazine in the presence of HCl, followed by addition of a dithiocarbamate (dtc) to give  $[\text{ReN}(\text{dtc})_2]$  [25]. To incorporate the nitride core, it is of interest to synthesize complexes with a mixed ligand system analogous to a  $[3 + 2]$  systems, which have been shown to be effective for oxo complexes. The same approach for the nitrides gives mixtures of compounds, however, it has been shown that the stereochemistry and stoichiometry of the Tc or Re nitride cores can be controlled using tridentate SNS or PNP donors. In the case of PNP ligands, the  $\pi$ -acceptor P donors favor a *trans* geometry [26]. The halide ligands are placed in a *cis* position and they can readily be substituted by bidentate monoanionic or dianionic ligands [27]. This control level can be achieved with bidentate nitrogen ligands (i.e. bipy, phenanthroline) that allow the isolation of the cyanonitrido complexes [28]. The use of bulky thiolate ligands demonstrated stabilizing effect on the rhenium nitride, arylimido and nitrile cores [29].

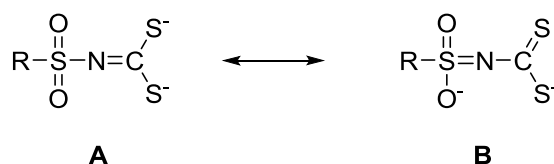
The structure of the Re dichloride (compound **E**) and the cationic dithiocarbamate derivative bis[(dimethoxypropylphosphanyl)ethyl]ethoxyethylamine  $\text{N,N}'$ -bis(ethoxyethyl) dithiocarbamate nitrido technetium(V), Tc-*N*-DBDOC (compound **F** which shows promise as a cardiac imaging agent *in vivo*) are shown in Fig. 1[30]. A choice of bidentate ligands with bioorthogonal functionalization can lead to conjugation to a range of biomolecules as well as high kinetic stabilities [31–35].

Rhenium has two beta-emitting radioisotopes,  $^{186}\text{Re}$  and  $^{188}\text{Re}$ , and through careful ligand design these can be encapsulated and then targeted to cancer cells where the beta-radiation emitted destroys the cancer cells. Both of these species are reactor-produced radioisotopes which are attractive for a variety of therapeutic applications. Thus far, Re-186 is unavailable from a generator system, and must therefore be directly produced in a nuclear reactor.

However, Re-188 can be eluted as perrhenate from an alumina-based  $^{188}\text{W}/^{188}\text{Re}$  generator, and although it has a much shorter half-life of 16.9 h, this is still compatible with most *in vivo* imaging and therapy requirements as it emits a beta-particle with a much higher energy (2.12 MeV and a 155 keV gamma photon, 15%) which would be also suitable for the coupled SPECT imaging.

To date, the majority of research into rhenium based therapeutic agents design has centered around the rhenium(V) oxo core. Our approach in this study was to investigate the coordination of a series of sulfonyl-dithiocarbamate ligands to the rhenium(V) nitride,  $[\text{Re}\equiv\text{N}]^{2+}$  core. This work focuses on the synthesis and coordination behavior of sulfonamide based dithiocarbamates (Scheme 2, **SDTC 1–4**) towards the rhenium(V) nitride core. The aim here is to functionalize the dithiocarbamate backbone by incorporating both fluorescent and non-fluorescent aromatic groups in the sulfonamide substituent. This will enable observation of the behavior of these complexes at the cellular level. To date, the only related rhenium compounds reported in the literature are neutral and involve the diethyldithiocarbamate ligand [36,37].

A measure of water solubility is a prerequisite for metal complexes to be used in biomedical applications. A commonly adopted approach is to add polar groups containing carboxylate, hydroxy or sulfonate groups to the ligand backbone. Here, we have adopted an alternate approach by using sulfonyl substituted dithiocarbamate ligands. Dithiocarbamate ligands have been relatively little studied and there have been just a couple of X-ray structures reported of Re complexes, readily prepared from sulfonamides and  $\text{CS}_2$  in the presence of a base [38,39]. They have two possible resonance forms as shown in Scheme 1. In form *B*, one negative charge resides on a sulfonyl oxygen giving a charged group closely related to the sulfonic acids ( $\text{RSO}_3^-$ ). We anticipate that such complexes could be water-soluble and this would be enhanced by a negative charge on the complex.

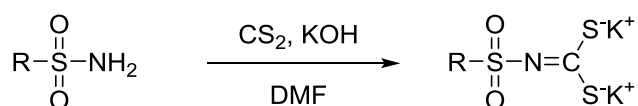


**Scheme 1.** Proposed resonance forms for dithiocarbamate-based ligands.

The substituents on the sulfonyl backbone of the ligands, methyl, phenyl, tolyl and naphthyl groups, have been carefully chosen in the work reported hereby to improve kinetic stabilities and modulate the lipophilicities. To enhance the understanding of the behavior of these compounds in cells across a range of conditions and concentration domains, a fluorescent ligand tag (e.g. naphthyl based) is desirable as it would allow the monitoring of the *in vitro* behavior of the compound. The design and synthesis of a series of ligands and of their novel complexes are here reported. Currently there are no reports in the literature regarding X-ray structures of Re complexes with this ligand. New species were characterized in solution and in the solid state, and their UV–Vis spectroscopy behavior in solution was investigated. The fluorescence spectra of a new naphthyl-tagged ligand and investigations into its corresponding Re(V) complex are also reported. A stability study of the tolyl complex,  $[\text{ReN}(\text{SDTC}_2)_2]^{2-}$ , in the presence of water over a period of 6 h was also conducted showing promising kinetic stability compatible with its intended pre-clinical aims. The complex proved to be stable in the presence of  $\text{H}_2\text{O}$ , with the UV–Vis spectra showing little change over this period.

## Results and Discussions

The synthesis of the sulfonamide dithiocarbamate ligands was adapted from literature procedures [36,37] and successfully employed for all starting materials with alkylic and aryllic backbones. The addition of carbon disulfide to the sulfonamides in a basic medium yielded the dianionic dithiocarbamate ligands as potassium salts (Scheme 2).



R: phenyl **SDTC1**  
tolyl **SDTC2**  
methyl **SDTC3**  
naphthyl **SDTC4**

**Scheme 2.** General synthesis for dithiocarbamate ligands.

A significant fluorescence emission was observed for the dianionic ligand with the naphthyl backbone (denoted SDTC4) with excitation and emission in the UV region of the spectrum (Fig. 1). Interestingly, the excitation and emission spectra also showed peaks of lower intensity in the NIR region (650–700 nm). The fluorescence emission in this region is especially attractive for biomedical imaging as interference from tissue autofluorescence *in vitro* and *in vivo* substantially decreases in the NIR.

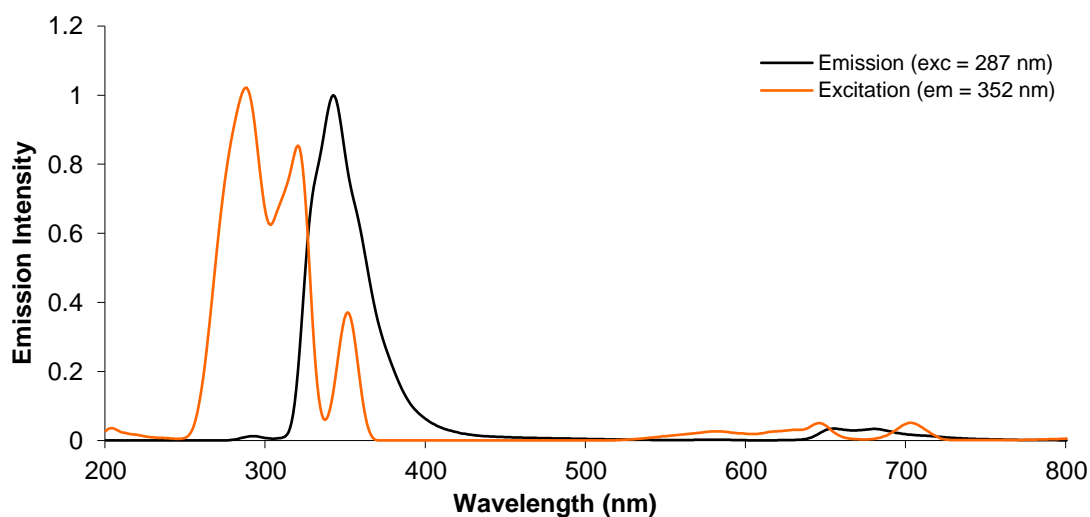
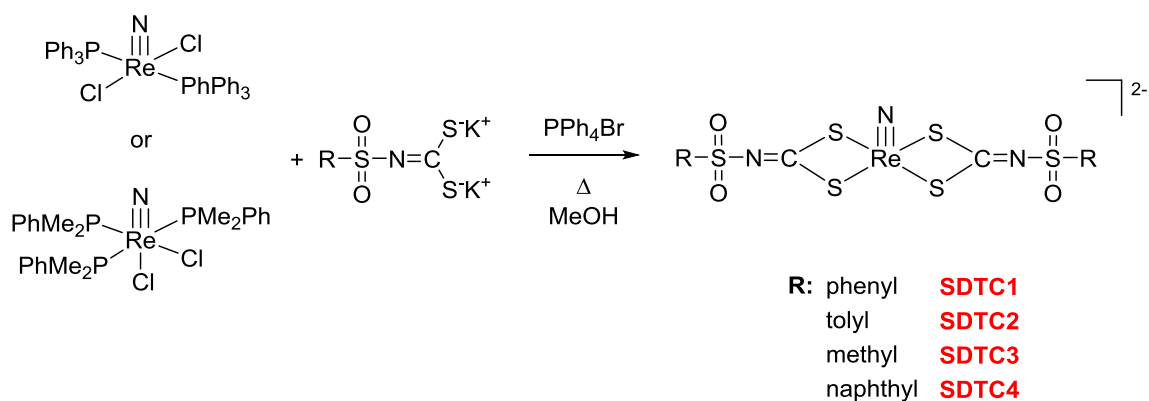


**Figure 2.** Normalized excitation (black line) and emission (orange line) spectra of ligand [SDTC4] $\text{K}_2$  in  $\text{CH}_3\text{CN}/\text{H}_2\text{O}$ .



**Scheme 3.** General procedure for the preparation of  $[\text{ReN}(\text{SDTC})_2][\text{PPh}_4]_2$  complexes anions. The two  $[\text{PPh}_4]^+$  counterions were omitted in the scheme shown above.

The reaction of the ligands with rhenium nitride precursors results in bis-substitution of the dithiocarbamate ligand, and in the formation of a dianionic rhenium(V) complex of the type  $[\text{ReN}(\text{SS})_2]^{2-}$  (Scheme 3).

The desired complexes featuring the  $[\text{ReN}]^{2+}$  (Re(V)) core were obtained either from the  $[\text{ReNCl}_2(\text{PPh}_3)_2]$  or  $[\text{ReNCl}_2(\text{PPhMe}_2)_3]$  by refluxing in methanol with the ligands and adding  $\text{PPh}_4\text{Br}$  to generate the counter-ion. The negative ESI TOF mass spectra obtained for the  $[\text{ReN}(\text{SDTC3})_2]^{2-}$  complex show peaks for the protonated complex,  $[\text{M}+\text{H}]^-$ , but also for the dianionic species,  $m/z$  corresponding to  $[\text{M}]^{2-}$ . The ESI TOF results obtained for the complex  $[\text{ReN}(\text{SDTC4})_2]^{2-}$ , however, only showed the dianionic species  $[\text{M}]^{2-}$  (see ESI).

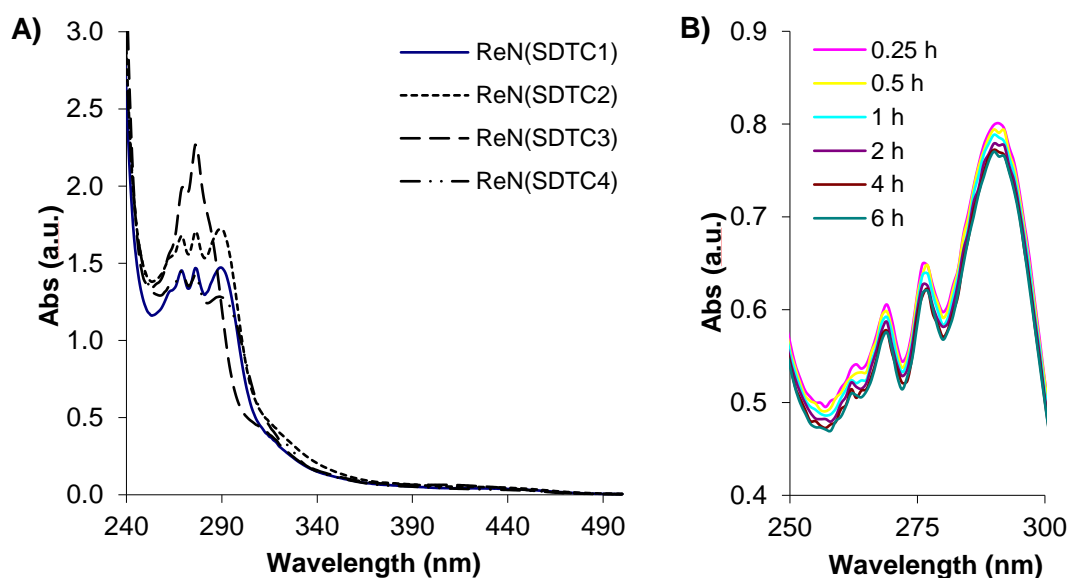


**Figure 3.** A) UV-vis spectra of Re nitride complexes in  $\text{CH}_3\text{CN}$  (10 mM conc); B) Stability tests of  $[\text{ReN}(\text{SDTC2})_2][\text{PPh}_4]_2$  by UV-Vis spectroscopy in aqueous  $\text{CH}_3\text{CN}$  (ca. 1:1  $\text{CH}_3\text{CN}:\text{H}_2\text{O}$ , 10 mM).

Furthermore, the UV–vis spectra of the prepared rhenium complexes are summarized in Fig. 3(A) as well as the corresponding stability test in aqueous media for  $[\text{ReN}(\text{SDTC4})_2][\text{PPh}_4]_2$  is given in Fig. 3(B). The absorption maxima is maintained at ca. 270–280 nm and in the case of SDTC4, the bands above 300 nm are not observed in the complex.

Interestingly, a search in the literature confirmed that the reported X-ray crystal structures for rhenium nitride complexes with bidentate S-donor ligands are scarce (*vide infra*). Among these, only a handful display a square pyramidal geometry like the compounds described herein. Other examples including those with additional phosphine ligands and adopting a pseudo-octahedral geometry [40–42] or multimetallic complexes [43–49] are outside the scope of this discussion and consequently not included here.

The closest examples to the complexes prepared in this work are depicted in Fig. 4. In all examples, the Re-N nitride distances are practically identical while the Re-S distances vary more with the type of ligands. The dithiolate derivative, **II**[15], presents the shorter Re-S distances followed by the complexes containing dithiocarbamate ligands, **I**[50] and  $[\text{ReN}(\text{SDTC1})_2][\text{PPh}_4]_2$ . The longer distances found are consistent with the likely occurrence of the canonical form *B* in Scheme 1. The complex with dithioimidophosphinato ligands, **IV**[19], presents the longest Re-S distances with values around 2.4 Å (Fig. 4). The ORTEP representation of the  $[\text{ReN}(\text{SDTC1})_2][\text{PPh}_4]_2$  complex acquired using synchrotron X-ray radiation is represented in Fig. 5 and a summary of the most representative structural parameters is listed in Table 1.

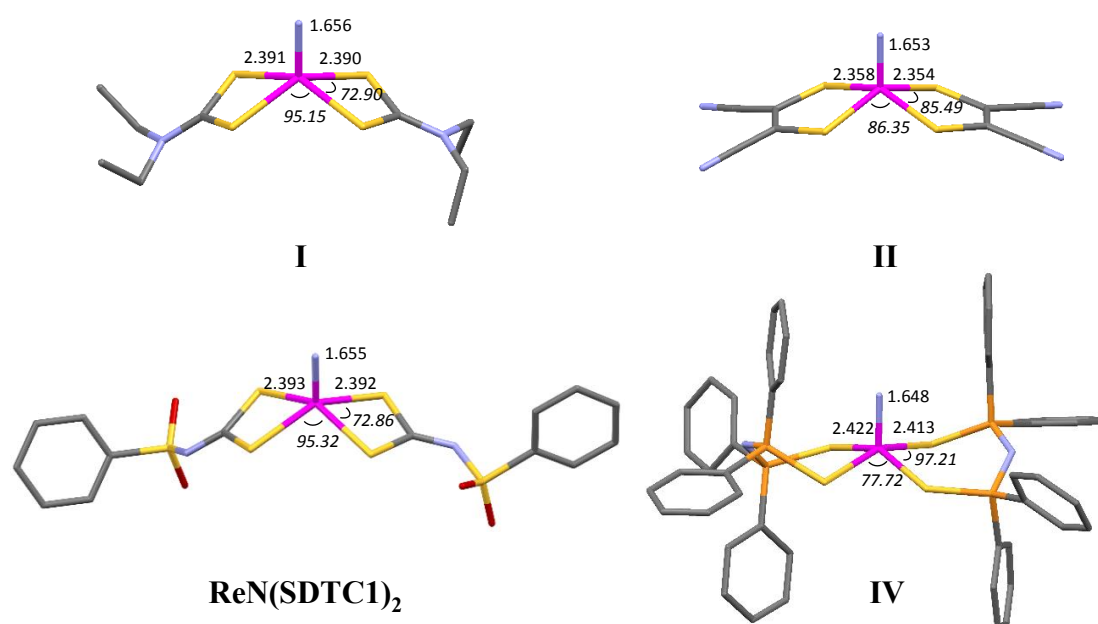


**Figure 4.** Distances (Å) and angles (*italics*, °) of ReN complexes including S donor ligands in a square pyramidal geometry. Hydrogen atoms have been omitted for clarity.

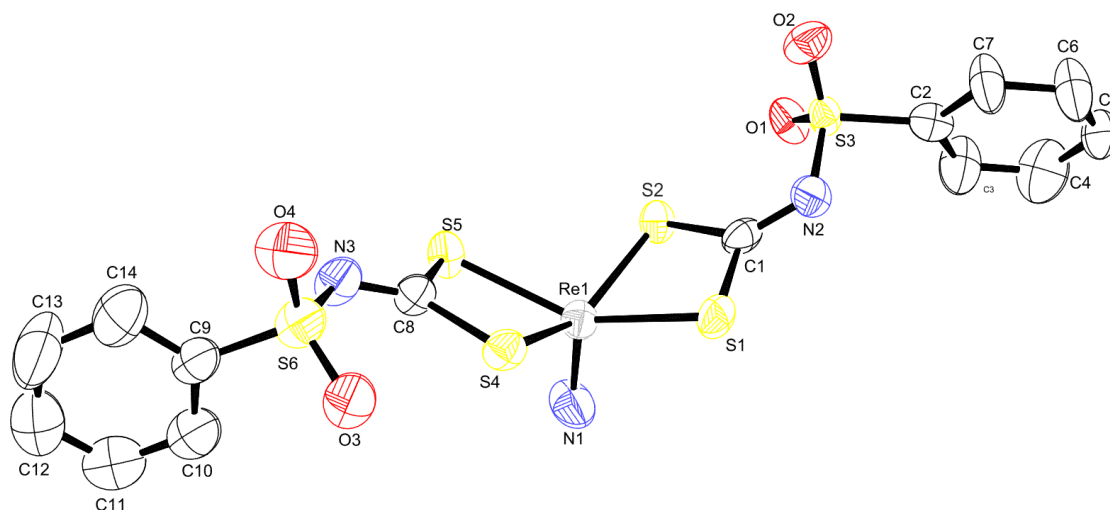


**Figure 5.** Synchrotron X-ray diffraction data ( $\lambda = 0.69110 \text{ \AA}$ ); molecular structure of  $[\text{ReN}(\text{SDTC1})_2][\text{PPh}_4]_2$ . Ellipsoids shown at the 50% level.  $\text{PPh}_4^+$  cations and hydrogen atoms have been omitted for clarity.

**Table 1.** Selected bond lengths and angles for the complex  $[\text{ReN}(\text{SDTC1})_2][\text{PPh}_4]_2$ .

Bond	Bond length ( $\text{\AA}$ )	Angle	Bond angles ( $^\circ$ )
Re1–N1	1.655(5)	N1–Re1–S1	108.2(2)
Re1–S1	2.373(1)	N1–Re1–S2	108.4(2)
Re1–S2	2.393(1)	N1–Re1–S4	106.1(2)
Re1–S4	2.368(1)	N1–Re1–S5	105.4(2)
Re1–S5	2.393(1)	S1–Re1–S2	72.86(4)
N2–C1	1.282(6)	S4–Re1–S5	72.98(4)
N3–C8	1.280(6)	S2–Re1–S4	145.48(5)
S1–C1	1.750(5)	S1–Re1–S5	146.27(5)
S2–C1	1.758(4)	S1–C1–S2	107.5(3)
S4–C8	1.754(5)	S4–C8–S5	107.2(3)
S5–C8	1.764(4)	C1–N2–S3	121.5(4)
		C8–N3–S6	121.9(4)

Additionally we carried out investigation by DFT calculations on the binding of the anionic ligands to the  $[\text{ReN}]^{2+}$  core. For the model ligand SDTC1, and the corresponding dianionic complex, gas phase DFT optimizations using a variety of basis sets under Gaussian platforms were employed. In each case, as expected for these bonding models, there are delocalized bonding throughout which appeared to be favored for both the experimental structure and the model compounds. The optimized (Fig. 6, Table 2 and ESI) geometries are in agreement with the findings from X-ray diffraction studies on  $[\text{ReN}(\text{SDTC1})_2][\text{PPh}_4]_2$  and other literature data [15,19,50] and Figs. 4 and 5.

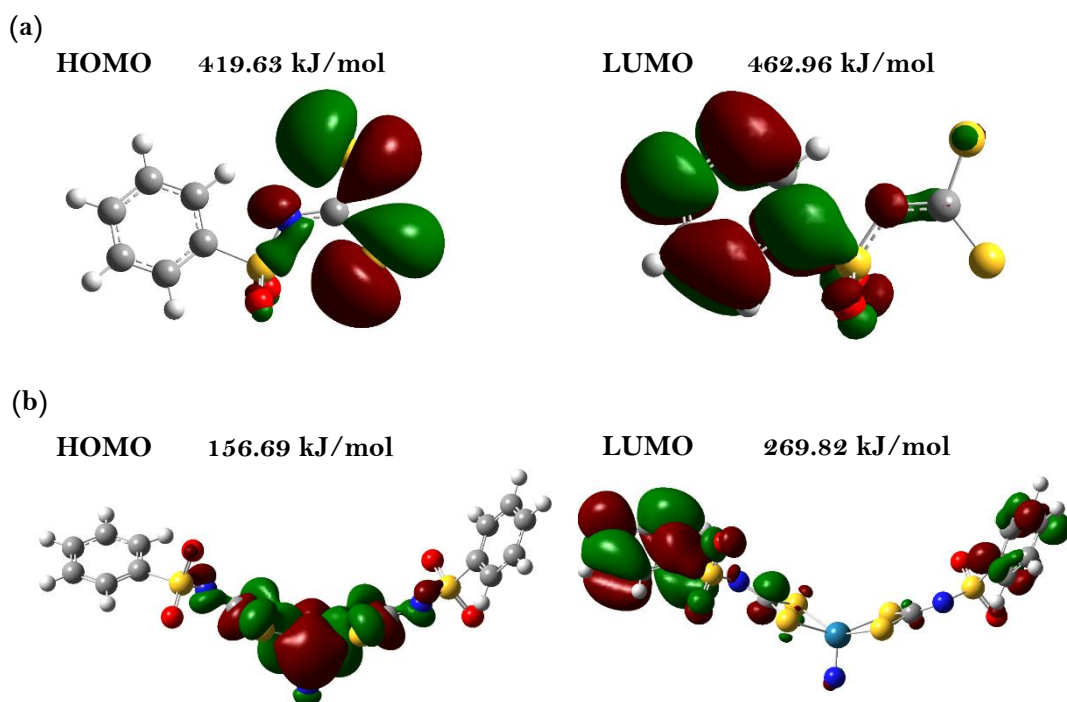


**Figure 6.** DFT calculated energies and shapes of selected frontier orbitals (HOMO and LUMO) for (a)  $[(\text{SDTC1})]^{2-}$  and (b)  $[\text{ReN}(\text{SDTC1})_2]^{2-}$ . Additional frontier orbitals and their energies are given in ESI. Structures optimized in the gas phase using the exchange correlation functional PBE/PBE LANL2TZ/631G\*\* basis set.

**Table 2.** DFT Calculated bond lengths and angles for the anion complex  $[\text{ReN}(\text{SDTC1})_2]^{2-}$  using the PBE/PBE exchange correlation function and two different basis sets. Additional conditions surveyed are given in ESI.

Bond	Bond length (Å)		Angle	Bond angles (°)	
	LANL2TZ/ 6-31G**	aug- cc-PVTZ pp/ 6-31G**		LANL2TZ /6-31G**	aug- cc- PVTZ pp/ 6-31G**
Re1-N1	1.669	1.665	N1-Re1-S1	107.17	107.32
Re1-S1	2.421	2.411	N1-Re1-S2	106.74	106.95
Re1-S2	2.426	2.415	N1-Re1-S4	106.88	106.82
Re1-S4	2.424	2.417	N1-Re1-S5	107.20	107.32
Re1-S5	2.419	2.412	S1-Re1-S2	72.62	72.65
N2-C1	1.324	1.325	S4-Re1-S5	72.67	72.63
N3-C8	1.323	1.325	S2-Re1-S4	146.38	146.24
S1-C1	1.775	1.774	S1-Re1-S5	145.62	145.35
S2-C1	1.771	1.769	S1-C1-S2	108.08	107.65
S4-C8	1.772	1.769	S4-C8-S5	107.94	107.65
S5-C8	1.776	1.774	C1-N2-S3	123.38	122.80

Key structural data for the experimental structure, species modelled as well as the partial charge distributions estimated are also given in the Supporting Information.

Molecular parameters are in agreement with those resulting from the X-ray structural data and the calculated IR spectra  $[\text{STDC1}]^{2-}$  and  $[\text{ReN}(\text{STDC1})_2]^{2-}$  also support the assignments made for the experimental IR spectra (ESI). The shapes and energies for the frontier orbitals for the  $[\text{STDC1}]^{2-}$  and  $[\text{ReN}(\text{STDC1})_2]^{2-}$  (DFT-calculated, Fig. 6) are also given. These are of interest to explore in the context of the fact that UV–Vis spectroscopy of the Re(V) compound could be observed experimentally and showed strong absorption bands in the 250–350 nm region of the spectrum. Encouraged by these calculations the involvement of such frontier orbitals in the transitions responsible for fluorescence emission spectra was also evaluated. Whilst for the simple complexes bearing the  $[\text{SDTC1}]$ – $[\text{SDTC3}]$  anionic ligands the fluorescence was rather weak, the fluorescence emission spectrum of the potassium salt of the SDTC4 free ligand was observed (Fig. 2 and ESI). Interestingly, the fluorescence emission quenching upon metallation with Re(V) and the formation of the  $[\text{ReN}(\text{SDTC4})_2]^{2-}$  complex dianion occurred in  $\text{CH}_3\text{CN}$  solutions (ESI). This loss of fluorescence emission may well be as a result of non-radiative pathways due to the dynamic equilibria between canonical forms *A/B* (shown in Scheme 1) of the coordinating ligand becoming involved in solutions. Also, the presence of traces of paramagnetic rhenium species forming in aerated solution during the analysis could not be fully discounted at first, therefore the kinetic stability tests in aqueous environment were carried out: spectroscopic evaluations of compounds of this class showed a remarkable kinetic stability in water media (Fig. 3B). The complex  $[\text{ReN}(\text{SDTC2})_2]^{2-}$  proved to be stable in  $\text{CH}_3\text{CN}:\text{H}_2\text{O}$  with the UV–Vis spectra showing little change over this period. Taking the shape and energies of HOMO-LUMO calculated by DFT for SDTC1 and  $[\text{ReN}(\text{SDTC1})_2]^{2-}$  in the simplified gas phase models (using a wide variety of basis sets and conditions, ESI), it is feasible to assume that these frontier orbitals are involved in the observed electronic absorption bands and in the occurrence of fluorescence [51]. The higher energy gap between the HOMO and LUMO orbitals in the complex compared to the ligand can indicate that the metal-to-ligand charge transfer associated to the fluorescence process is not as favored resulting in a quenching of the fluorescence intensity. Furthermore, the stability study of the tolyl complex,  $[\text{ReN}(\text{SDTC2})_2]^{2-}$  monitored in an organic solvent ( $\text{CH}_3\text{CN}$ ) in the presence of water over a period of 6 h was also conducted showing promising kinetic stability compatible with its intended pre-clinical aims. Longer term we are interested in setting the foundations for the Re(V) radiochemistry labelling which requires aqueous conditions. As such, prior to engaging in extensive ‘hot’ experiments using  $^{186/188}\text{Re}$  we have been establishing the ‘cold’ chemistry protocols hereby, and fluorescence spectroscopy proved to be a helpful tool in assessing the necessary compatibility and kinetic stability in aqueous solutions.

## Conclusions and outlook

The synthesis of new ligands and their  $[\text{ReN}]^{2+}$  core-tagged complexes was described herein. The characterization data in solution and in the solid state as well as the crystal structure of the metal complex  $[\text{ReN}(\text{SDTC1})_2](\text{PPh}_4)_2$  are given. This compound is representative of the series and incorporates the phenyl sulfonamide backbone: its geometry was discussed and compared to DFT level gas-phase calculations. Additional highlights are the fact that the free dianionic ligand SDTC4 isolated as a potassium salt is fluorescent in wet solvents, however, it is clear that quenching has taken place upon its coordination to the Re(V) centre. New coordination chemistry of Re(V) in wet organic solvents was developed hereby and opens up the possibility of generating complexes including the  $[\text{S}(\text{O})_2\text{N}]$  moiety known for playing a role in the

selective reductive trapping of related compounds in hypoxic cells and tissues: further work in this context is currently in progress in our laboratories.

### Experimental Section

The rhenium precursors  $[\text{ReNCl}_2(\text{PPh}_3)_2]$ , and  $[\text{ReNCl}_2(\text{PMe}_2\text{Ph})_3]$  were prepared according to literature procedures.[7, 52] These complexes were fully characterized and used in further reactions to give the desired metallic sulfonamide based dithiocarbimates.

#### General procedure for sulfonamide dithiocarbamate synthesis

Ligands SDTC1 to SDTC4 as dipotassium salts were prepared following literature procedures.[37, 38] Generally, carbon disulfide (1 eq.) and KOH (1 eq.) were added to the sulfonamide starting material (1 eq.) dissolved in DMF. The reaction was stirred at 0 °C for 2 h and a second equivalent of KOH added and the mixture further stirred for 1 h. The removal of the solvent resulted in the precipitation of the dithiocarbamate salts as pale yellow solids.

**Dipotassium (phenylsulfonyl)carbonimidodithioate (SDTC1):** Yield: 51%. Anal. Calc. for  $\text{C}_7\text{H}_5\text{S}_3\text{O}_2\text{NK}_2 \cdot 2\text{H}_2\text{O}$ : C, 24.3; H, 2.6, N, 4.0%. Found: C, 24.1; H, 2.4; N, 3.9%.  $^1\text{H}$  NMR ( $d^6$ -DMSO):  $\delta$  7.28-7.34 (m, 3H); 7.65-7.72 (m, 2H). IR ( $\text{cm}^{-1}$ ): 1263 ( $\nu\text{CN}$ ); 1253 ( $\nu\text{SO}_{2\text{ass}}$ ); 1132 ( $\nu\text{SO}_{2\text{sym}}$ ); 978 ( $\nu\text{CS}_2$ ).

**Dipotassium (tosyl)carbonimidodithioate (SDTC2):** Yield: 94%. Anal. Calc. for  $\text{C}_8\text{H}_7\text{S}_3\text{O}_2\text{NK}_2 \cdot 3\text{H}_2\text{O}$ : C, 25.4; H, 3.5; N, 3.7%. Found: C, 25.1; H, 2.9; N, 3.7%.  $^1\text{H}$  NMR ( $d^6$ -DMSO):  $\delta$  7.57 (d,  $J = 8.0$  Hz, 2H); 7.06 (d,  $J = 8.0$  Hz, 2H); 2.26 (s,  $\text{CH}_3$ ). IR ( $\text{cm}^{-1}$ ): 1267 ( $\nu\text{CN}$ ); 1256 ( $\nu\text{SO}_{2\text{ass}}$ ); 1136 ( $\nu\text{SO}_{2\text{sym}}$ ); 973 ( $\nu\text{CS}_2$ ).

**Dipotassium (methyl)carbonimidodithioate (SDTC3):** Yield: 60%.  $^1\text{H}$  NMR ( $d^6$ -DMSO):  $\delta$  2.98 (s, 3H). IR ( $\text{cm}^{-1}$ ): 1287 ( $\nu\text{CN}$ ); 1265 ( $\nu\text{SO}_{2\text{ass}}$ ); 1187 ( $\nu\text{SO}_{2\text{sym}}$ ); 960 ( $\nu\text{CS}_2$ ).

**Dipotassium (naphthylsulfonyl)carbonimidodithioate (SDTC4):** Yield 83 %. Anal. Calc. for  $\text{C}_{11}\text{H}_7\text{S}_3\text{O}_2\text{NK}_2 \cdot \text{H}_2\text{O}$ : C, 35.0; H, 2.4; N, 3.7%. Found: C, 34.5; H, 2.6; N, 3.3%.  $^1\text{H}$  NMR ( $d^6$ -DMSO):  $\delta$  8.40 (s, 1H), 8.15 – 8.04 (m, 2H), 8.01 (d,  $J = 7.5$  Hz, 1H), 7.88 (d,  $J = 8.6$  Hz, 1H), 7.71 – 7.59 (m, 2H). IR ( $\text{cm}^{-1}$ ): 1273 ( $\nu\text{CN}$ ), 1264 ( $\nu\text{SO}_{2\text{ass}}$ ), 1144 ( $\nu\text{SO}_{2\text{sym}}$ ), 971 ( $\nu\text{CS}_2$ ).

#### General procedure for the synthesis of sulfonamide dithiocarbamate rhenium nitride complexes

$\text{ReNCl}_2(\text{PPh}_3)_2$  (0.120 g, 0.151 mmol) was added to  $[\text{SDTC1}]\text{K}_2$  (0.164 g, 0.530 mmol) in methanol (50 mL) and the resulting solution was heated under reflux for a period of 4 h. To the orange/brown solution obtained,  $\text{PPh}_4\text{Br}$  (0.128 g, 0.305 mmol) was added in 3 mL of methanol. The solution was filtered, the solvent removed under vacuum, and the residue re-dissolved in 25 mL of dichloromethane. This solution was washed with  $\text{H}_2\text{O}$  and the organic layer dried over  $\text{MgSO}_4$ . The addition of an excess of diethyl ether yielded yellow precipitates, which in each case was washed with diethyl ether and dried under vacuum.

$[\text{ReN}(\text{SDTC4})_2](\text{PPh}_4)_2$  complex was isolated in a yield lower than 10% and characterized by mass spectrometry, IR, UV-Vis and fluorescence spectroscopies.

$[\text{ReN}(\text{SDTC1})_2](\text{PPh}_4)_2$ : The complex was prepared following the general procedure from  $\text{ReNCl}_2(\text{PPh}_3)_2$ , yield: 45 %. Anal. Calc. for  $\text{C}_{62}\text{H}_{50}\text{S}_6\text{O}_4\text{P}_2\text{N}_3\text{Re}$ : C, 55.5; H, 3.8; N, 3.1. Found: C, 55.2; H, 3.8; N, 3.1%.

Alternatively, this rhenium complex was prepared starting from  $\text{ReNCl}_2(\text{PMe}_2\text{Ph})_3$  precursor and following the same experimental protocol. The same product was obtained. Yield: 90 %. Anal. Calc. for  $\text{C}_{62}\text{H}_{50}\text{S}_6\text{O}_4\text{P}_2\text{N}_3\text{Re} \cdot \text{H}_2\text{O}$ : C, 54.8; H, 3.9; N, 3.1%. Found: C, 54.4; H, 3.8; N, 3.0%.

**[ReN(SDTC2)<sub>2</sub>](PPh<sub>4</sub>)<sub>2</sub>**: The complex was prepared following the general procedure, from ReNCl<sub>2</sub>(PPh<sub>3</sub>)<sub>2</sub>, yield: 57 %. From ReNCl<sub>2</sub>(PMe<sub>2</sub>Ph)<sub>3</sub>, yield: 45 %. Anal. Calc. for C<sub>64</sub>H<sub>54</sub>S<sub>6</sub>O<sub>4</sub>P<sub>2</sub>N<sub>3</sub>Re: C, 56.1; H, 4.0; N, 3.1. Found: C, 56.3; H, 3.9; N, 2.8%.

**[ReN(SDTC3)<sub>2</sub>](PPh<sub>4</sub>)<sub>2</sub>**: The complex was prepared following the general procedure from ReNCl<sub>2</sub>(PPh<sub>3</sub>)<sub>2</sub>, yield: 57 %. From ReNCl<sub>2</sub>(PMe<sub>2</sub>Ph)<sub>3</sub>, yield: 45 %. Anal. Calc. for C<sub>52</sub>H<sub>46</sub>S<sub>6</sub>O<sub>4</sub>P<sub>2</sub>N<sub>3</sub>Re·4H<sub>2</sub>O: C, 48.4; H, 4.2; N, 3.3; S, 14.9%. Found: C, 48.1; H, 3.9; N, 3.6; S, 15.2%.

### Crystal Structure Determination

Crystals suitable for X-ray crystallography were obtained from the slow evaporation of a methanol solution of the complex at room temperature. The crystals were isolated by filtration, and a specimen crystal was selected under an inert atmosphere, covered with polyfluoroether and mounted on the end of a glass fibre.

Crystallographic data for **[ReN(SDTC1)<sub>2</sub>](PPh<sub>4</sub>)<sub>2</sub>** were collected at the SRS Daresbury Radiation Source. The crystal structure was deposited at the Cambridge Crystallographic Data Centre. The data have been assigned to the deposition numbers: **CCDC 1561939** contains the supplementary crystallographic data for this paper. These data can be obtained free of charge from The Cambridge Crystallographic Data Centre via [www.ccdc.cam.ac.uk/data\\_request/cif](http://www.ccdc.cam.ac.uk/data_request/cif). The asymmetric unit consists of 1.5 Re-complex molecules and three PPh<sub>4</sub> cationic species as counterions. One generally well-ordered formula unit is 2(C<sub>24</sub>H<sub>20</sub>P)(C<sub>14</sub>H<sub>10</sub> N<sub>3</sub>O<sub>4</sub>ReS<sub>6</sub>). The Re complex with Re2 atom is located on a centre of inversion, with Re2 and N2 disordered over two sites which were refined with 50% occupation. One tosyl-group in the complex with Re1 shows disorder over two sites in the ratio 54:46. Three out of four phenyl groups attached to P3 are disordered over two sites and were modelled with geometric constraints.

Unit cell Parameters: a= 10.3136(2) Å, b= 14.3596(3) Å, c= 58.1686(14) Å, beta= 92.0450(10)°, space group P2<sub>1</sub>/n, Z=6, V= 8609.2(3) Å<sup>3</sup>, T= 150(2) K, μ= 2.158mm<sup>-1</sup>; Formula weight 1341.55, 67942 reflections measured (Rint 0.073); Data/restraints/parameters: 22882 / 12 / 1214. Final R indices [I>2σ(I)] Full-matrix least-squares refinement on F<sup>2</sup>: R<sub>1</sub> = 0.0560 and wR<sub>2</sub> = 0.1461. R indices (all data) R<sub>1</sub> = 0.0733 and wR<sub>2</sub> = 0.1533.

### DFT Calculations

All calculations were carried out using density functional theory with different exchange correlation functionals (B3LYP, B3PW91, BVP86, HSEH1PBE, MPW1PW91 and PBEPBE) as implemented in the Gaussian 09 package.[54] Different basis sets (SDD, LANL2DZ, 6311+G\*, 631G\*\*, LANL2TZ, aug-cc-PVTZ-pp, Def2 TZVPPD, HAY WADT MBN1ECP and dhf TZVPP) were used to get the accurate geometries of [STDC1]<sup>2-</sup> and [ReN(STDC1)<sub>2</sub>]<sup>2-</sup> closer to the experiment. Calculated bond lengths and bond angles using different combinations of exchange correlation functionals and basis sets together with the experimental values are given in the electronic supplementary information. All geometry optimizations were performed without symmetry constraints. Vibrational frequencies were calculated on the optimized structures and were scaled using a scaling factor of 0.986. Mulliken[55] and natural[56] population analysis were carried out to estimate the charges on each atoms. Molecular orbital diagrams were generated using GaussView 6.0.16 visualization program included in the Gaussian 09 package.

## Acknowledgements

STFC is thanked for funding this work via access to synchrotron facilities. Dr John Warren is thanked for assistance with data collection. Mass spectrometry EPSRC service at Swansea is thanked for support, as is the Imperial College EPSRC Supercomputing Facility. The ERC Consolidator Grant O2Sense to S.I.P. and EPSRC CDT and CSCT Centre at Bath University are thanked for financial support.

---

## References

- [1] M.B. Mallia, A.S. Shinto, M. Kameswaran, K.K. Kamaleswaran, R. Kalarikal, K.K. Aswathy, S. Banerjee, *Cancer Biother. Radiopharm.*, 31 (2016) 139-144.
- [2] R. Alberto, *Compr. Coord. Chem. II*, 5 (2004) 127-270.
- [3] U. Abram, *Compr. Coord. Chem. II*, 5 (2004) 271-402.
- [4] (a) J.R. Dilworth, S.I. Pascu, *The Radiopharmaceutical Chemistry of Technetium and Rhenium*, in: *The Chemistry of Molecular Imaging*, John Wiley & Sons, Inc, 2014, pp. 137-164; (b) J. R Dilworth, S. I Pascu, P. A Waghorn, D. Vullo, S. R Bayly, M. Christlieb, X. Sun, C. T Supuran, *Dalton Transactions* 44(11), (2015), 4859-4873.
- [5] J.R. Dilworth, P.S. Donnelly, *75Re Therapeutic Rhenium Radiopharmaceuticals*, in: *Metallotherapeutic Drugs and Metal-Based Diagnostic Agents*, John Wiley & Sons, Ltd, 2005, pp. 463-487.
- [6] J. Chatt, J.D. Garforth, N.P. Johnson, G.A. Rowe, *J. Chem. Soc.*, (1964) 1012-1020.
- [7] J. Chatt, C.D. Falk, G.J. Leigh, R.J. Paske, *J. Chem. Soc. (A)*, (1969) 2288-2293.
- [8] J. Baldas, J. Bonnyman, *J. Nucl. Med. Allied Sci.*, 29 (1985) 187-187.
- [9] J. Kanellos, G.A. Pietersz, I.F.C. McKenzie, J. Bonnyman, J. Baldas, *JNCI: Journal of the National Cancer Institute*, 77 (1986) 431-439.
- [10] G.A. Williams, J. Bonnyman, J. Baldas, *Aust. J. Chem.*, 40 (1987) 27-33.
- [11] G.A. Williams, J. Baldas, *Aust. J. Chem.*, 42 (1989) 875-884.
- [12] J. Baldas, *Pure Appl. Chem.*, 62 (1990) 1079-1080.
- [13] J. Baldas, J.F. Boas, J. Bonnyman, S.F. Colmanet, G.A. Williams, *Inorg. Chim. Acta*, 179 (1991) 151-154.
- [14] J. Baldas, *Technetium and Rhenium*, 176 (1996) 37-76.
- [15] U. Abram, M. Braun, S. Abram, R. Kirmse, A. Voigt, *J. Chem. Soc., Dalton Trans.*, (1998) 231-238.
- [16] U. Abram, S. Abram, H. Spies, R. Kirmse, J. Stach, K. Kohler, *Z. Anorg. Allg. Chem.*, 544 (1987) 167-180.
- [17] U. Abram, B. Lorenz, L. Kaden, D. Scheller, *Polyhedron*, 7 (1988) 285-289.
- [18] J.R. Dilworth, R. Hubener, U. Abram, *Z. Anorg. Allg. Chem.*, 623 (1997) 880-882.
- [19] U. Abram, E. Schulz Lang, S. Abram, J. Wegmann, J. R. Dilworth, R. Kirmse, J. Derek Woollins, *J. Chem. Soc., Dalton Trans.*, (1997) 623-630.
- [20] A. Boschi, A. Duatti, L. Uccelli, *Development of Technetium-99m and Rhenium-188 Radiopharmaceuticals Containing a Terminal Metal–Nitrido Multiple Bond for Diagnosis and Therapy*, in: W. Krause (Ed.) *Contrast Agents III: Radiopharmaceuticals – From Diagnostics to Therapeutics*, Springer Berlin Heidelberg, Berlin, Heidelberg, 2005, pp. 85-115.
- [21] R. Pasqualini, A. Duatti, *J. Chem. Soc., Chem. Commun.*, (1992) 1354-1355.
- [22] R. Pasqualini, E. Bellande, V. Comazzi, A. Duatti, *Eur. J. Nucl. Med.*, 19 (1992) 593-593.
- [23] A. Boschi, A. Massi, L. Uccelli, M. Pasquali, A. Duatti, *Nucl. Med. Biol.*, 37 (2010) 927-934.
- [24] A. Duatti, A. Marchi, R. Pasqualini, *J. Chem. Soc., Dalton Trans.*, (1990) 3729-3733.

- [25] F. Demaimay, A. Roucoux, N. Noiret, H. Patin, *J. Organomet. Chem.*, 575 (1999) 145-148.
- [26] A. Boschi, E. Cazzola, L. Uccelli, M. Pasquali, V. Ferretti, V. Bertolasi, A. Duatti, *Inorg. Chem.*, 51 (2012) 3130-3137.
- [27] C. Bolzati, A. Boschi, A. Duatti, S. Prakash, L. Uccelli, F. Refosco, F. Tisato, G. Bandoli, *J. Am. Chem. Soc.*, 122 (2000) 4510-4511.
- [28] W. Purcell, H.G. Visser, *Transition Met. Chem.*, 40 (2015) 899-906.
- [29] P.J. Blower, J.R. Dilworth, *J. Chem. Soc., Dalton Trans.*, (1985) 2305-2309.
- [30] C. Cittanti, L. Uccelli, M. Pasquali, A. Boschi, C. Flammia, E. Bagatin, M. Casali, M. Stabin, L. Feggi, M. Giganti, A. Duatti, *J. Nucl. Med.*, 49 (2008) 1299-1304.
- [31] C. Decristoforo, I. Santos, H.J. Pietzsch, J.U. Kuenstler, A. Duatti, C.J. Smith, A. Rey, R. Alberto, E. Von Guggenberg, R. Haubner, Q. J. Nucl. Med. Mol. Imaging, 51 (2007) 33-41.
- [32] C. Bolzati, A. Mahmood, E. Malagò, L. Uccelli, A. Boschi, A.G. Jones, F. Refosco, A. Duatti, F. Tisato, *Bioconjugate Chem.*, 14 (2003) 1231-1242.
- [33] A. Boschi, L. Uccelli, A. Duatti, C. Bolzati, F. Refosco, F. Tisato, R. Romagnoli, P.G. Baraldi, K. Varani, P.A. Borea, *Bioconjugate Chem.*, 14 (2003) 1279-1288.
- [34] A. Boschi, C. Bolzati, E. Benini, E. Malagò, L. Uccelli, A. Duatti, A. Piffanelli, F. Refosco, F. Tisato, *Bioconjugate Chem.*, 12 (2001) 1035-1042.
- [35] F. Refosco, C. Bolzati, A. Duatti, F. Tisato, L. Uccelli, *Recent Res. Dev. Inorg. Chem.*, 2 (2000) 89-98.
- [36] J.F. Rowbottom, G. Wilkinson, *J. Chem. Soc., Dalton Trans.*, (1972) 826-830.
- [37] U. Abram, S. Ritter, *Inorg. Chim. Acta*, 210 (1993) 99-105.
- [38] P.D. Howes, J.J. Payne, M. Pianka, *J. Chem. Soc., Perkin Trans. 1*, (1980) 1038-1044.
- [39] L.M. Gomes Cunha, M.M. Magalhães Rubinger, J.R. Sabino, L.L.Y. Visconte, M.R. Leite Oliveira, *Polyhedron*, 29 (2010) 2278-2282.
- [40] L. H. Doerrer, A. J. Graham, M. L. H. Green, *J. Chem. Soc., Dalton Trans.*, (1998) 3941-3946.
- [41] U. Abram, A. Voigt, R. Kirmse, *Polyhedron*, 19 (2000) 1741-1748.
- [42] S. Ritter, U. Abram, *Inorg. Chim. Acta*, 231 (1995) 245-248.
- [43] U. Abram, A. Hagenbach, A. Voigt, R. Kirmse, *Z. Anorg. Allg. Chem.*, 627 (2001) 955-964.
- [44] H. Zheng, W.-H. Leung, J.L.C. Chim, W. Lai, C.-H. Lam, I.D. Williams, W.-T. Wong, *Inorg. Chim. Acta*, 306 (2000) 184-192.
- [45] S. Ritter, U. Abram, *Z. Anorg. Allg. Chem.*, 622 (1996) 965-973.
- [46] D.V. Griffiths, S.J. Parrott, M. Togrou, J.R. Dilworth, Y. Zheng, S. Ritter, U. Abram, *Z. Anorg. Allg. Chem.*, 624 (1998) 1409-1414.
- [47] J.B. Stelzer, A. Hagenbach, U. Abram, *Z. Anorg. Allg. Chem.*, 628 (2002) 703-706.
- [48] U. Abram, *Z. Anorg. Allg. Chem.*, 626 (2000) 318-320.
- [49] U. Abram, *Z. Anorg. Allg. Chem.*, 625 (1999) 839-841.
- [50] S.R. Fletcher, A.C. Skapski, *J. Chem. Soc., Dalton Trans.*, (1972) 1079-1082.
- [51] J. P. Holland, F. I. Aigbirhio, H. M. Betts, P. D. Bonnitcho, P. Burke, M. Christlieb, G. C. Churchill, A. R. Cowley, J. R. Dilworth, P. S. Donnelly, J. C. Green, J. M. Peach, S. R. Vasudevan and J. E. Warren, *Inorg. Chem.*, 2007, **46**, 465-485.
- [52] J. Chatt, J.D. Garforth, N.P. Johnson, G.A. Rowe, *Journal of the Chemical Society (Resumed)*, (1964) 1012-1020.
- [53] M. J. Frisch *et al.*, *Gaussian 09* (Gaussian, Inc., Wallingford CT, 2009)
- [54] R. S. Mulliken, *J. Chem. Phys.*, 23 (1955) 1833-1840.
- [55] R. B. Weinstock and F. Weinhold, *J. Chem. Phys.*, 83:2 (1985) 735-746.